



Original Article

Microstructural evolution and microhardness in a low carbon steel processed by high-pressure torsion[☆]



Diana Maritza Marulanda Cardona^{a,*}, Jittraporn Wongsan-Ngam^b, Terence G. Langdon^c

^a Research Group in Energy and Materials (REM), Faculty of Mechanical Engineering, Universidad Antonio Nariño, Bogotá, Colombia

^b Department of Mechanical Engineering, Faculty of Engineering, King Mongkut's Institute of Technology Ladkrabang, Bangkok 10520, Thailand

^c Materials Research Group, Faculty of Engineering and the Environment, University of Southampton, Southampton, United Kingdom

ARTICLE INFO

Article history:

Received 10 June 2014

Accepted 30 September 2014

Available online 6 November 2014

Keywords:

Hardness

High-pressure torsion

Homogeneity

Low carbon steel

ABSTRACT

A low-carbon triple-alloyed steel was processed by high-pressure torsion at room temperature for up to 5 turns under a pressure of 6.0 GPa. Microhardness, scanning electron microscopy and X-ray diffraction were used to investigate the hardness and microstructural evolution of the steel. Values of the Vickers microhardness were recorded across the sample diameters. The results show that there is a gradual evolution in both the hardness and the microstructure with increasing numbers of turns. However, the microhardness does not become fully homogeneous across the sample diameter after five turns and there remain significantly lower values in the center of the disk. These results indicate that complete homogeneity across the disks for this steel requires applied pressures higher than 6.0 GPa and/or torsional straining through more than 5 turns.

© 2014 Brazilian Metallurgical, Materials and Mining Association. Published by Elsevier Editora Ltda. Este é um artigo Open Access sob a licença de [CC BY-NC-ND](http://creativecommons.org/licenses/by-nc-nd/4.0/)

1. Introduction

The bulk properties of a material are of great importance for engineering applications. Comprehensive investigations on techniques for improving these properties are crucial, especially for materials for technological use such as with the iron-carbon system and its alloys [1]. Among these, the AISI 8620 low carbon – triple-alloyed steel is of great interest because of its use in manufacturing as a gear material and for

hard-wearing machine parts when it is hardened and formed through carburizing or boronizing [2].

Improving the mechanical properties of this steel requires the use of techniques that modify its internal structure. Among these techniques, processing by high-pressure torsion (HPT) has attracted attention because of the capacity for achieving exceptional grain refinement, often to the nanometer level, and exceptionally high strength [3]. It was shown recently that HPT processing causes grain refinement and the decomposition of a supersaturated solid solution [1].

[☆] Paper presented in the form of an abstract as part of the Proceedings of the Pan American Materials Conference, São Paulo, Brazil, July 21st to 25th 2014.

* Corresponding author.

E-mail: dmarulanda@uan.edu.co (D.M. Marulanda).

<http://dx.doi.org/10.1016/j.jmrt.2014.09.004>

2238-7854/© 2014 Brazilian Metallurgical, Materials and Mining Association. Published by Elsevier Editora Ltda.

Este é um artigo Open Access sob a licença de [CC BY-NC-ND](http://creativecommons.org/licenses/by-nc-nd/4.0/)

The aim of this study was to investigate the microstructural evolution and the corresponding changes in microhardness of the AISI 8620 steel subjected to processing by HPT. This steel has fractions of ferrite and pearlite which are expected to deform during the processing operation.

2. Experimental materials and procedures

The material used in this work was a low carbon – triple-alloyed steel containing 0.2% C, 0.5% Cr, 0.6% Ni, 0.2% Mo, 0.8 Mo with the balance as Fe where the composition is expressed in wt.%. The as-received material in the normalized state was machined to cylindrical rods of 10 mm diameter and 50 mm length. HPT disks with thicknesses of ~1 mm were sliced from the rod and these disks were polished to final thicknesses of ~0.86 mm. The samples were heat treated at a temperature of 650 °C for 15 min in order to relieve the stresses introduced by machining. It was anticipated that this treatment would not produce any significant changes in the material structure or mechanical properties.

The HPT processing was conducted under quasi-constrained conditions [4,5] using a facility consisting of upper and lower anvils having central depressions with diameters of 10 mm and depths of 0.25 mm [6]. The processing was conducted at room temperature by rotating the lower anvil at a speed of 1 rpm under an applied load of ~470 kN, which is equivalent to an imposed pressure of $P=6.0$ GPa. Separate disks were processed through totals of $N=1/4$, 1, 2 and 5 turns. Two disks were prepared for each condition, for microstructure and microhardness measurements. The upper surface of each disk was marked immediately after HPT and prior to any microstructural analysis and hardness measurements.

Following HPT, X-ray diffraction patterns of the processed disks were recorded using an X'PertPro Panalytical diffractometer working with the following settings: θ - 2θ varying from 10° to 90° with 0.02° step size, monochromatic CuK α radiation ($\lambda = 1.5409$ Å), 45 kV and 40 mA. For microhardness measurements, each processed disk was mounted and polished to have a mirror-like surface and measurements were taken at positions separated by 0.3 mm across the diameters of each disk with four individual points recorded around each selected position at distances of 0.15 mm. Full details of this procedure were given in an earlier report [7]. The microhardness measurements were taken using an Esseyway model 600 hardness tester at a load of 50 kg-F and 20 s dwell time.

For microstructural observation using scanning electron microscopy (SEM), the disks were polished to have a mirror-like surface and then they were etched with nital solution. Images were taken using a JEOL model JSM 6490-LV SEM working at 10 kV near the mid-radius positions at distances of ~2 and ~4 mm from the center of each disk.

3. Results and discussion

Fig. 1 shows the X-ray diffraction patterns of the samples processed to different numbers of turns. Only the ferrite phase in orientations (1 1 0), (2 0 0) and (2 1 1) is observed according to the JCPDS 00-006-0696 database. Diffraction peaks of pearlite

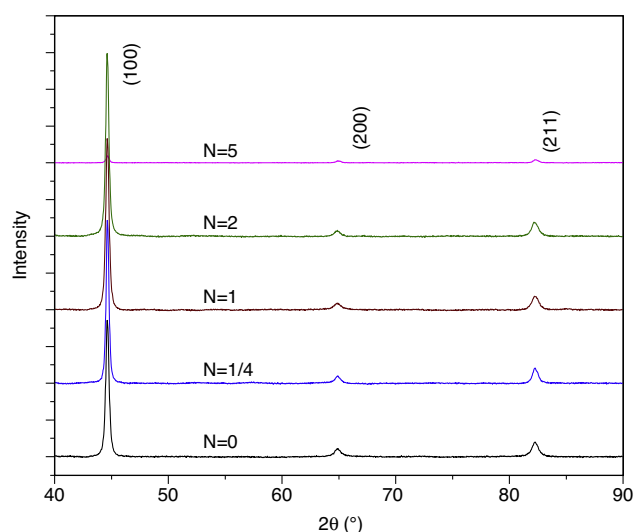


Fig. 1 – X-ray diffraction patterns for the samples processed through different numbers of turns.

were not present due to its low volume fraction in this steel. It is readily apparent that no phase transformation occurs after the HPT process. However, there is a change in the peak intensities after five turns that indicates the occurrence of microstructural changes due to the formation of nanostructures and the dissolution of the pearlite lamella in the steel [8,9]. On the other hand, the full width at half maximum of the peaks does not show a significant variation and this is probably because the patterns were taken at the centers of the disks in the low deformation zone.

Fig. 2 shows images of the surfaces of the samples processed through different numbers of rotations in HPT. These images were recorded near the mid-radius position at a distance of ~2 mm from the center of the disk. It can be seen that the structure at this position after 1/4 and 1 turn is not highly deformed and the microstructural features of ferrite and pearlite, shown in dark and bright contrast respectively, are clearly visible. At this stage, the soft ferrite grains were probably deformed by dislocation subdivision [10]. This type of SPD-induced grain refinement was reported earlier in ferrite [9]. After 2 revolutions in Fig. 2(c) ferrite and pearlite are present in the form of elongated grains and the spacing of the cementite lamella has decreased. The original grain boundaries appear to have been essentially compressed and they are elongated in the direction of grain flow with the thickness of the grains decreasing with increasing strain [11]. This characteristic of elongated grains is expected when deformed by a shear strain, even in the early stages of deformation [8]. After five turns in Fig. 2(d), no clear patterns or structural features are observed. This is probably due to the development of a very small grain size and the deformation of pearlite that occurs by further decreasing the interlamellar distance to form a structure of alternate ferrite and carbon enriched areas [12].

Fig. 3 shows images recorded at a distance of ~4 mm from the centers of the disks. Microstructural changes are observed at this position even after processing for only 1/4 revolution. After 1 revolution in Fig. 3(b), the pearlite is highly deformed

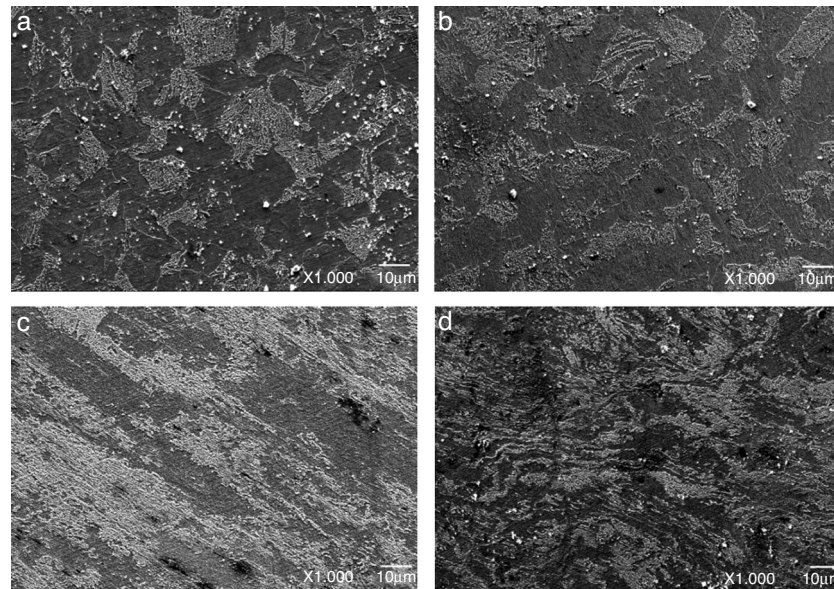


Fig. 2 – Images by SEM of the structures at ~2 mm of the mid-radius position after processing through different numbers of turns. (a) After 1/4 turn, (b) after 1 turn, (c) after 2 turns, (d) after 5 turns.

and microstructural refinement is observed by decreasing the initial interlamellar distance. The microstructural refinement continues at 2 turns in Fig. 3(c). After 5 turns in Fig. 3(d), no clear patterns are observed for the structural features and this is attributed to the development of the very small grain size and the dissolution of cementite in the ferrite matrix.

The distributions of microhardness along the diameters of the HPT disks for different numbers of rotations are shown in Fig. 4. The hardness for the steel before processing is shown as the lower line labeled $N=0$ with an average value of 173 ± 5 Hv, which is comparable for the values reported for commercial normalized AISI 8620 steel. After 1/4 revolution in Fig. 4(a), the microhardness values change from 260 HV in the central

region to approximately 400 HV at the edge of the disk. This type of distribution of microhardness values is in good correlation with investigations related with microhardness evolution in different metals [13,14] and is due to the variation in strain across the disk during HPT processing.

The microhardness values after 1 revolution in Fig. 4(b) increase significantly at the edge of the sample but in the central region only a minor increase is observed. In this condition, the hardness values have reached approximately 490 HV at the edge of the disk. After 2 revolutions in Fig. 4(c), there is a moderate increase in the hardness values at the edge of the disk but there is also a gradual increase in the hardness values in the mid-radius and central regions. Thus, the hardness has

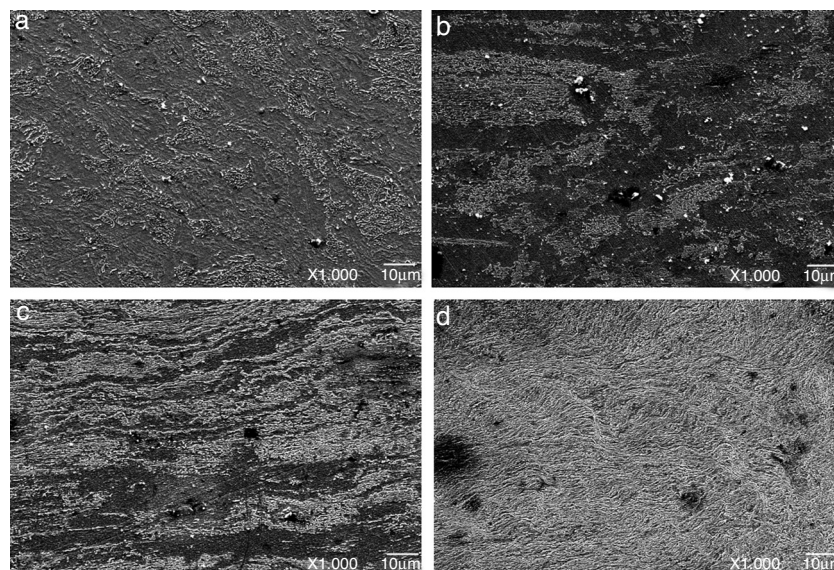


Fig. 3 – Images by SEM of the structures at ~4 mm of the mid-radius positions after processing through different numbers of turns. (a) After 1/4 turn, (b) after 1 turn, (c) after 2 turns, (d) after 5 turns.

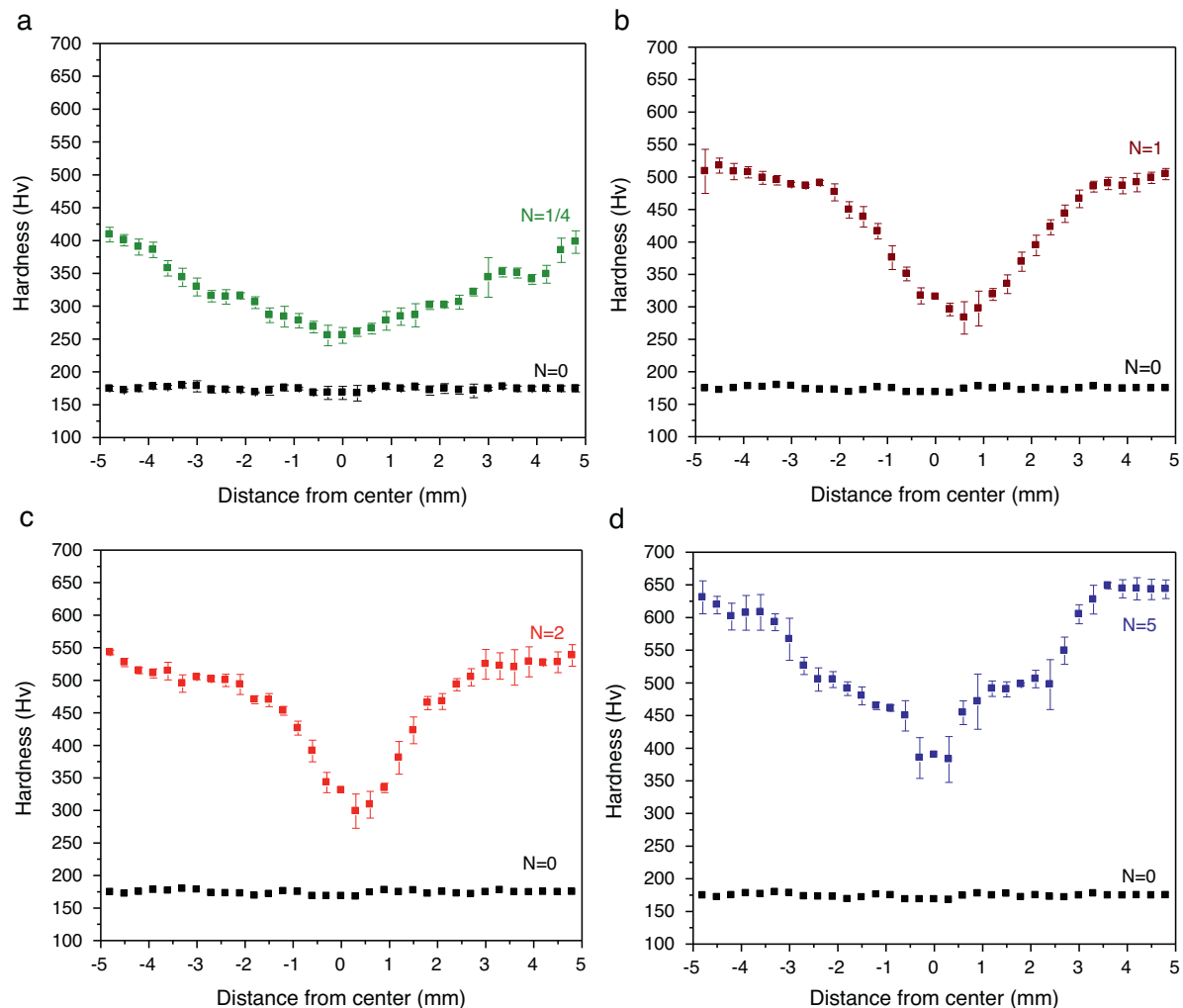


Fig. 4 – Microhardness profiles after processing through different numbers of turns. (a) After 1/4 turn, (b) after 1 turn, (c) after 2 turns, (d) after 5 turns.

increased to approximately 320 HV in the central part and to about 530 HV at the edge.

For the sample deformed through 5 revolutions in Fig. 4(d), there is a significant increase in the microhardness values along the radial directions. The hardness increases to approximately 400 HV in the central region and 620 HV at the edge of the disk. It is also observed that there is a high inhomogeneity in microhardness distribution along the diameter of the disk. This indicates that the microhardness has not reached the saturation condition. In the saturation regime, the deformation-induced refinement is in equilibrium with the deformation-induced coarsening by grain boundary migration so that there is no further microstructural refinement or changes in the mechanical properties [15].

From these results, it appears that the microstructural refinement, as observed in Figs 2 and 3, has not reached the saturation regime and this indicates that complete homogeneity across the disks for this steel requires applied pressures higher than 6.0 GPa and/or torsional straining through more than 5 turns. On the other hand, there is evidence that the alloying elements present in this steel may reduce the saturation grain size [15], but nevertheless the steel

has not reached the saturation microstructure to attain an overall homogeneity in hardness [16].

4. Summary and conclusions

1. High-pressure torsion (HPT) was used to process a low carbon-low alloyed AISI 8620 steel and the microstructure and microhardness were recorded after processing through 1/4 to 5 turns.
2. There is a gradual evolution in both microstructure and microhardness after HPT processing but the microhardness values fail to reach a homogeneous distribution along the sample diameter after 5 turns.
3. It is concluded that full homogeneity of the microstructure across the disks for this steel, and therefore of the microhardness, requires applied pressures higher than 6.0 GPa and/or torsional straining through more than 5 turns.

Conflicts of interest

The authors declare no conflicts of interest.

Acknowledgments

One of the authors gratefully acknowledges the financial support of the Universidad Antonio Nariño, Colombia, through project number 2011-242, “Nanostructured Steels Obtained by Severe Plastic Deformation” (DMM). This work was supported in part by the European Research Council under ERC Grant Agreement No. 267464-SPDMETALS.

REFERENCES

- [1] Straumal BB, Mazilkin AA, Protasova SG, Dobatkin SV, Rodin AO, Baretzky B, et al. Fe-C nanograined alloys obtained by high-pressure torsion: structure and magnetic properties. *Mater Sci Eng A* 2009;503:185–9.
- [2] Tabur M, Izciler M, Gul F, Karacan I. Abrasive wear behavior of boronized AISI 8620 steel. *Wear* 2009;266: 1106–12.
- [3] Zhilyaev AP, Langdon TG. Using high-pressure torsion for metal processing: fundamentals and applications. *Prog Mater Sci* 2008;53:893–979.
- [4] Figueiredo RB, Cetlin PR, Langdon TG. Using finite element modeling to examine the flow processes in quasi-constrained high-pressure torsion. *Mater Sci Eng A* 2011;528:8198–204.
- [5] Figueiredo RB, Pereira PHR, Aguilar MTP, Cetlin PR, Langdon TG. Using finite element modeling to examine the temperature distribution in quasi-constrained high-pressure torsion. *Acta Mater* 2012;60:3190–8.
- [6] Wongs-Ngam J, Kawasaki M, Zhao Y, Langdon T. Microstructure evolution and mechanical properties of a Cu–Zr alloy processed by high-pressure torsion. *Mater Sci Eng A* 2011;528:7715–22.
- [7] Kawasaki M, Langdon TG. The significance of strain reversals during processing by high-pressure torsion. *Mater Sci Eng A* 2008;498:341–8.
- [8] Belyakov A, Kimura Y, Tsuzaki K. Microstructure evolution in dual-phase stainless steel during severe deformation. *Acta Mater* 2006;54:2521–32.
- [9] Song R, Ponge D, Raabe D, Speer JG, Matlock DK. Overview of processing, microstructure and mechanical properties of ultrafine bcc steels. *Mater Sci Eng A* 2006;441:1–17.
- [10] Cao Y, Wang YB, An HX, Liao XZ, Kawasaki M, Ringer SP, et al. Concurrent microstructural evolution of ferrite and austenite in a duplex stainless steel processed by high-pressure torsion. *Acta Mater* 2014;63:16–29.
- [11] Narayana Murthy SVS, Torizuka S, Nagai K, Koseki N, Kogo Y. Classification of microstructural evolution during large strain high Z deformation of a 0.15 C carbon steel. *Scr Mater* 2005;52:713–8.
- [12] Kammerhofer C, Hohenwarter A, Scheriau S, Brantner HP, Pippan R. Influence of morphology and structural size on the fracture behavior of a nanostructured pearlitic steel. *Mater Sci Eng A* 2013;585:190–6.
- [13] Kawasaki M, Figueiredo RB, Langdon TG. An investigation of hardness homogeneity throughout disks processed by high-pressure torsion. *Acta Mater* 2011;59:308–16.
- [14] Korznikova EA, Mironov SYu, Korznikov AV, Zhilyaev AP, Langdon TG. Microstructural evolution and electro-resistivity in HPT nickel. *Mater Sci Eng A* 2012;556:437–45.
- [15] Pippan R, Scheriau S, Taylor A, Hafok M, Hohenwarter A, Bachmaier A. Saturation of fragmentation during severe plastic deformation. *Ann Rev Mater Res* 2010;40:319–43.
- [16] Pippan R, Wetscher F, Hafok M, Vorhauer A, Sabirov I. The limits of refinement by severe plastic deformation. *Adv Eng Mater* 2006;8:1046–56.